Virtual Screening for SARS-CoV Protease Based on KZ7088 Pharmacophore Points†

Suzanne Sirois,[‡,§] Dong-Qing Wei,[§,||,⊥] Qishi Du,[||] and Kuo-Chen Chou*[,||,#]

Départment de chimie, Université du Québec à Montréal (UQAM), C.P. 8888 Succursale Centre-Ville, Montréal, Québec, Canada H3C 3P8, Institut Technologique de Montreal, Suite 168, 5253 boul. Decarie, Montreal, Quebec, Canada H3W 3C3, Tianjin Institute of Bioinformatics and Drug Discovery (TIBDD) and Tianjin Normal University, Tianjin, China 300074, Center for Research in Molecular Modeling, Concordia University, Montreal, Canada, and Gordon Life Science Institute, San Diego, California 92130

Received November 18, 2003

Pharmacophore modeling can provide valuable insight into ligand−receptor interactions. It can also be used in 3D (dimensional) database searching for potentially finding biologically active compounds and providing new research ideas and directions for drug-discovery projects. To stimulate the structure-based drug design against SARS (severe acute respiratory syndrome), a pharmacophore search was conducted over 3.6 millions of compounds based on the atomic coordinates of the complex obtained by docking KZ7088 (a derivative of AG7088) to SARS CoV M^{pro} (coronavirus main *pro*teinase), as reportedly recently (Chou, K. C.; Wei, D. Q.; Zhong, W. Z. *Biochem. Biophys. Res. Commun.* **2003**, *308*, 148−151). It has been found that, of the 3.6 millions of compounds screened, 0.07% are with the score satisfying five of the six pharmacophore points. Moreover, each of the hit compounds has been evaluated for duggability according to 13 metrics based on physical, chemical, and structural properties. Of the 0.07% compounds thus retrieved, 17% have a perfect score of 1.0; while 23% with one druggable rule violation, 13% two violations, and 47% more than two violations. If the criterion for druggability is set at a maximum allowance of two rule violations, we obtain that only about 0.03% of the compounds screened are worthy of further tests by experiments. These findings will significantly narrow down the search scope for potential compounds, saving substantial time and money. Finally, the featured templates derived from the current study will also be very useful for guiding the design and synthesis of effective drugs for SARS therapy.

I. INTRODUCTION

SARS is a viral respiratory illness caused by a previously unrecognized coronavirus, called SARS-associated coronavirus (SARS-CoV). Reported first in Asia in February 2003, the illness spread within only a few months to more than two dozen countries in North America, South America, Europe, and Asia. The patient suffering from SARS usually begins with a high fever, sometimes associated with chills or other symptoms, such as headache, body aches, and diarrhea, followed by developing a dry, nonproductive cough that might be accompanied by or progress to a condition (hypoxia) in which insufficient oxygen is getting to the blood. Most patients develop pneumonia. The virus that causes SARS is mainly spread by respiratory droplets produced when an infected person coughs or sneezes. The virus can also spread through person-to-person contact. In addition to the "droplet spread" and "person-to-person contact spread", SARS-CoV might also be spread through the air, the so-called "airborne spread", or by other ways that are not quite known yet. Although the SARS global outbreak of 2003 was contained, it is possible that the disease could reemerge, causing even greater disaster because the viruses might occur in many different mutated forms. In view of this, it is a critical challenge to find effective drugs to inhibit the replication of SARS-CoV before it ever attacks human beings again. So far only a few treatments have been used against SARS, such as treatment by ribavirin, steroids, and alfacon-1. Earlier this year, almost all SARS patients in Hong Kong were treated with a combination of the antiviral drug ribavirin and steroids. However, many health experts thought that the efficacy of such a combination was unproved yet and might lead to some serious side effects.[1] Recently, it has been reported that dozens of former SARS patients in Hong Kong are suffering from bone degeneration, known as avascular necrosis, throwing the spotlight back on the controversial "cocktail of drugs" used to treat many patients during the epidemic. Because of these recent outcomes, it is vitally important to find drugs that effectively inhibit a known target of the SARS virus. The present study represents a part of continued efforts for the discovery of SARS-CoV protease inhibitors.

In this study we applied the pharmacophore model and virtual (in silico) screening in order to gain useful insights on ligand−receptor interactions for SARS CoV M^{pro} (coronavirus main proteinase) and to identify hit compounds that can eventually be modified to become lead candidates for drug. The term pharmacophore was originally defined as the 3D (dimensional) arrangement of atoms—or groups of atoms—responsible for the biological activity of a drug

* Corresponding author phone: (858)484-1018; fax: (858)484-1018; e-mail: kchou@san.rr.com.

† Abbreviations used: SARS, severe acute respiratory syndrome; CoV, coronavirus; M^{pro}, main proteinase.

‡ Université du Québec à Montréal (UQAM).

§ Institut Technologique de Montreal.

|| Tianjin Institute of Bioinformatics and Drug Discovery (TIBDD) and Tianjin Normal University.

⊥ Concordia University.

Gordon Life Science Institute.

10.1021/ci034270n CCC: $27.50
Published on Web 03/02/2004

Table 1. Physical, Chemical, and Structural Property Filters[11]

property filters	definition	min	max
# of hydrogen bond donors	Hdon	0	5
# of hydrogen bond acceptors	Hacc	0	10
molecular weight	MW	100	500
logP	SlogP	−2	5
# of rotatable bonds	#RotBond	0	15
# of rings	#Cycles > 6 (SSSR)	0	6
single chain length	SingleChain	0	7
ring size	BigRing	0	7
# of halogen atoms	#Halogen > 7	0	7
# of CF3CF2CF2	#CF3CF2CF2	0	1
# of nitrogen and oxygen atoms	#N&O	1	15

molecule. Pharmacophore models are constructed based on compounds of known biological activity and are refined as more data are acquired in an iterative process. The models can be used for optimizing a series of known ligands or, alternatively, they can be used to search molecular databases in order to find new structural categories—a process known as virtual screening. The virtual screening has become a cost-effective technology in search for novel lead compounds. Especially, availability of 3D structure of the target and the knowledge of its active site warrant us with sufficient accuracy to avoid doing the traditional high throughput screening by experiments, which is both time-consuming and costly. As a consequence, million of dollars can be saved because there is no need to buy costly HTS library of compounds and set up biological assays for the experimental screening. For example, a successful practice of the virtual screening was the Anthrax Research Project, in which a subset of about 300 000 molecules was identified as meriting further investigation from a pool of 3.5 billion of possible compounds, narrowing the search scope down to about 0.0086%.[2,3] It took only 24 days to complete the entire virtual screening project, a process which would have taken years and spent million of dollars to complete by means of the traditional experimental high-throughput screening.

II. MATERIALS AND METHODS

To expedite the drug-finding process, it is important to distinguish the differences that exist between drugs and nondrugs[4,5] so as to avoid wasting time to test compounds that are unlikely to be druggable. It is known that drugs candidates must satisfy certain rules that are quite different from other chemical classes of compounds.[5] Accordingly, those reactive compounds which do not satisfy certain physiochemical and structural guidelines can be safely rejected for further consideration. Based on such a rationale, a scoring function has been developed for druggable compounds.[4,6] In the present paper, a virtual screening based on pharmacophore point models was performed for both commercially and academic available compounds (see Table 3 for a complete list of suppliers). The operation was conducted with a novel scoring function (see eq 1 and 2) that takes into account physical,[7] chemical, and structural properties[8] as well as the presence of undesirable functional groups.[9,10] The selection of the properties was according to the work proposed by Baurin.[11] The software MOE (2002) from Chemical Computing Group of Montreal, Quebec, Canada was used to conduct pharmacophore searches (virtual screening) of potential hits.

Pharmacophore Points. Recently, the X-ray coordinates of SARS CoV M^{pro} (coronavirus main proteinase) determined by Anand et al.[12] were used by Chou et al.[13] as a targeted basis to conduct docking studies for KZ7088 and an octopeptide, respectively. The main proteinase consists of 304 amino acids, folded into three domains: domain 1 (res 8−99), domain 2 (res 100−183), and domain 3 (res 200−300). The binding cleft is located between domains 1 and 2. The ligand KZ7088 is a derivative of AG7088 (developed by Pfizer) by removing the −CH2 group from its fluorophenylalanine side chain. Seven pharmacophore points of KZ7088 are displayed in a recent paper.[13] The hydrogen bond donor and the acceptor are colored purple and cyan, respectively, whereas the aromatic group is colored green. The four hydrogen bond donors and the two hydrogen bond acceptors are responsible for forming the hydrogen bonds with the enzyme catalytic site as described by Chou et al.[13] Figure 2 shows the pharmacophore points of SARS-CoV interacting with KZ7088.[13] For every donor (key), there is an acceptor (lock) (purple-cyan pair), fully consistent with the docking result. Accordingly, it is anticipated that compounds satisfying those pharmacophoric points will have a high probability of being biologically active.

Druggability (Compound Scoring Functions). The scoring function developed here to assess druggability of CAC (commercially available compounds) is expressed in terms of 13 metrics as shown in Tables 1 and 2 as well as eq 1. The metrics includes identification of reactive functional groups defined by[9] the Lipinski's ROF (rule-of-five)[7] and structural descriptors as defined by Xu.[8] In Figure 1, the hydrogen bond donor is defined by OH and NH groups, whereas the hydrogen bond acceptor is defined by O and N atoms; logP is calculated according to Wildman and Crippen's definition,[14] which is named as SlogP in MOE;[15] cycles > 6[8] is the maximum SSSR size where SSSR is the smallest ring building block necessary to form other ring systems[8] and it describes molecular shape; CF3CF2CF2 is the number of perfluorinated chains; N&O is the number of N atoms and O atoms. It is instructive that Lipinski's ROF is a heuristic guide for determining if a compound will be orally bioavailable. The rules were derived from an analysis of 2245 compounds.[16] The assumption is that compounds meeting these criteria have entered human clinical trials and therefore must possess many of the desirable characteristics of drugs. An extension of these rules is the definition of a drug-like cluster center as presented by Xu.[8] It consists of a set of the distribution of selected structural descriptors derived from a database of existing drugs. With this definition the ROF descriptors are a subset of the drug-like cluster center. The 13 molecular properties metrics used to evaluate each compound are as follows:

$$\begin{aligned} \mathrm{MP} = \mathrm{reactive}^9 + \mathrm{MW}{>}500^7 + \mathrm{Hacc}{>}10^7 + \\ \mathrm{Hdon}{>}5^7 + \mathrm{logP}{>}5^7 + \mathrm{MW}{<}100 + \mathrm{Halogene}{>}7^8 + \\ \mathrm{CF3CF2CF2} + \mathrm{BigRing}{>}7^8 + \mathrm{RotBond}{>}15^8 + \\ (\mathrm{SSSR})\ \mathrm{cycles}{>}6^8 + \mathrm{SingleChain}{>}7^8 + \mathrm{N\&O}^8 \end{aligned} \quad (1)$$

The addition of these violation rules leads to the following form of the compound scoring function:

$$\mathrm{CompoundScore} = 1.0 - (0.1 \times \mathrm{MP}) \quad (2)$$

For each compound we have calculated the 13 metrics. For example: is the molecular weight of the compound greater than 500 (MW > 500)? If yes, 1 is entered into the column;

Table 2. Undesirable Functional Groups[9,10]

formyl halide	alkyl halide	isocyanate	vinyl ketone
acyl halide	anhydride	michael acceptor	O−O singlebond
formaldehyde	aziridine	perhalo-ketone	N−N singlebond
aldehyde	azide	phosphonate ester	S−O/S singlebond
aliphatic(thio)ester	1,2-dicarbonyl	sulfonate ester	N−O/S singlebond
aliphatic imine	epoxide	sulfonyl halide	b-heterocarbonyl
aliphatic ketone	halopyrimidine	thiol	phospho-
metal			

Table 3. List of Suppliers for Freely and Commercially Available Compounds

supplier	no. of compds	TableName	Web site
ACD	87657	ACD_Stock	www.acdlabschem.com
Akos	156140	Akos-Lithuania	www.akosgmbh.com
Akos	134465	Akos-Resynthetic	www.akosgmbh.com
Akos	28600	AkosOWH	www.akosgmbh.de
Asinex	129860	AsinexPlatinumMerge	www.asinex.com
Asinex	14240	AsinexPreformated	www.asinex.com
Asinex	194032	AsinexGoldMerge	www.asinex.com
Bionet (Ryan)	35080	Bionet	www.ryansci.com
ChemStar	85981	Chemstar	www.chemstaronline.com
ChemStar	40000	Chemstar_Plated	www.chemstaronline.com
Chembridge	30000	ChembridgeDVS	www.chembridge.com
Chembridge	321716	ChembridgeEx	www.chembridge.com
Chemical Diversity	175551	ChemDiv_CLab	www.chemdiv.com
Chemical Diversity	110484	ChemDiv_IDC	www.chemdiv.com
Comgenex	119247	Comgenex	www.comgenex.com
Enamine	109695	Enamine-RS	www.enamine.net
Enamine	124420	Enamine-S	www.enamine.net
Evotec	76817	Evotec_LeadDisc	www.evotecaoi.com
Evotec	122998	Evotec_Screening	www.evotecaoi.com
G&J (Ryan)	1867	GandJ	www.ryansci.com
IBS	195899	IBS n	www.ibscreen.com
IBS	172153	IBS s	www.ibscreen.com
IF Lab ltd	109400	IFlab	iflab@iflab.kiev.ua
KeyOrganics	34736	KeyOrganics	www.keyorganics.ltd.uk
Maybridge (Ryan)	75142	Maybridge	www.maybridge.com
MDPI	9367	MDPI	
Menai (Ryan)	4512	Menai	www.ryansci.com
Nanosyn	18613	NanosynExplore	www.nanosyn.com
Nanosyn	44000	NanosynPharma	www.nanosyn.com
NCI	126705	NCI_DTP	dtp.nci.nih.gov/docs/3d_database/structural_information/structural_data.html
Otava	104258	Otava Stock and Ya	
Peakdale	3770	Peakdale	www.peakdale.com
Pharmeks	84143	Pharmeks	www.pharmeks.com
Princeton BioMolecular Research	204215	Princeton	www.princetonbio.com
Ryan	1136	Ryan Intermediate	www.ryansci.com
Ryan	59214	Ryan Labo	www.ryansci.com
Sigma-Aldrich	13929	Sigma-Aldrich-L	www.sigma-aldrich.com
Sigma-Aldrich	69238	Sigma-Aldrich-R	www.sigma-aldrich.com
Sigma-Aldrich	46284	Sigma-Aldrich-S	www.sigma-aldrich.com
Sigma-Aldrich	58298	SigmaAldrich	www.sigma-aldrich.com
Specs Biospecs	172469	SPECS_10T	www.specsnet.com
Timtec	100276	Timtec_Stock	www.timtec.net
Timtec	9600	Timtec_MaxiVerse	www.timtec.com
Toslab	11743	Toslab collection + ugi	www.toslab.com
Tripos	87467	Tripos	http://leadquest.tripos.com
WorldMolecules	20401	WorldMolecules	www.worldmolecules.com

otherwise, 0. This means that a compound violates the druggable rule when its MW value is greater than 500. A summation is made over the 13 calculated metrics. Each metric has an equal weight of 0.1. Finally, the summation is deducted from 1.0. Compounds satisfying all the molecular property rules have a perfect score of 1.0 (eq 2).

III. RESULTS AND DISCUSSION

The results are presented by 2D virtual screening, 3D virtual screening, and seventh pharmacophore point, as given below.

2D Virtual Screening. The 2D hit compounds that were identified with virtual screening contain at least 5 of the 7 pharmacophore points (i.e., four H bond acceptors, two H bond donors, and one hydrophobic group), as shown in Figure 1. Most of the hit compounds retrieved are drug-like and satisfied the rules describe above. Table 4 contains the data obtained from the virtual screening. The number of compounds screened was over 3.6 million. The total number of unique 2D hits is 1584. The total number of 2D conformers is 2539. The hit ratio is 0.044%.

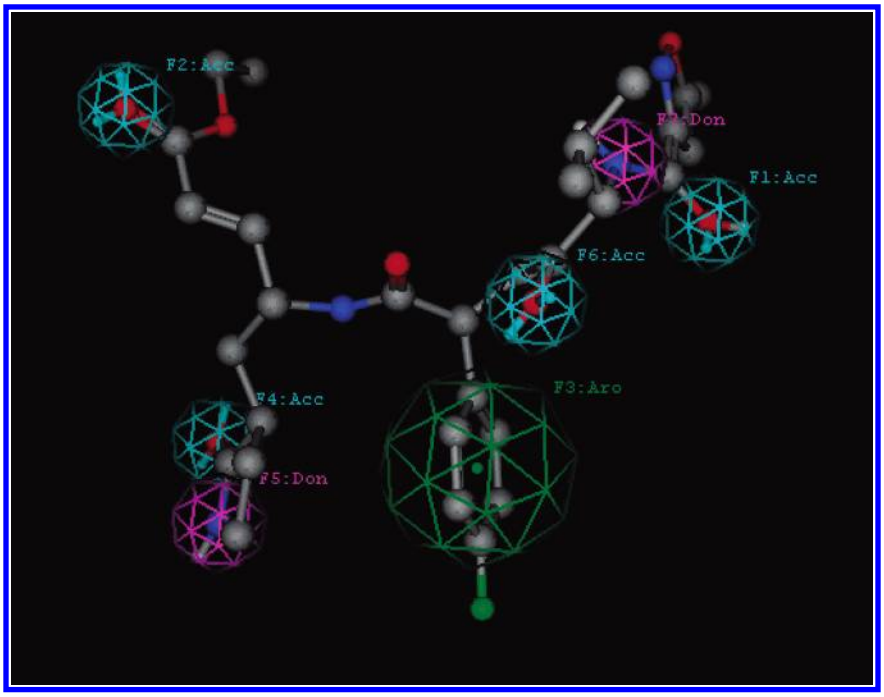

Figure 1. Seven pharmacophore points of KZ7088, where H bond acceptor is cyanic, H bond donor purple, and aromatic ring green.

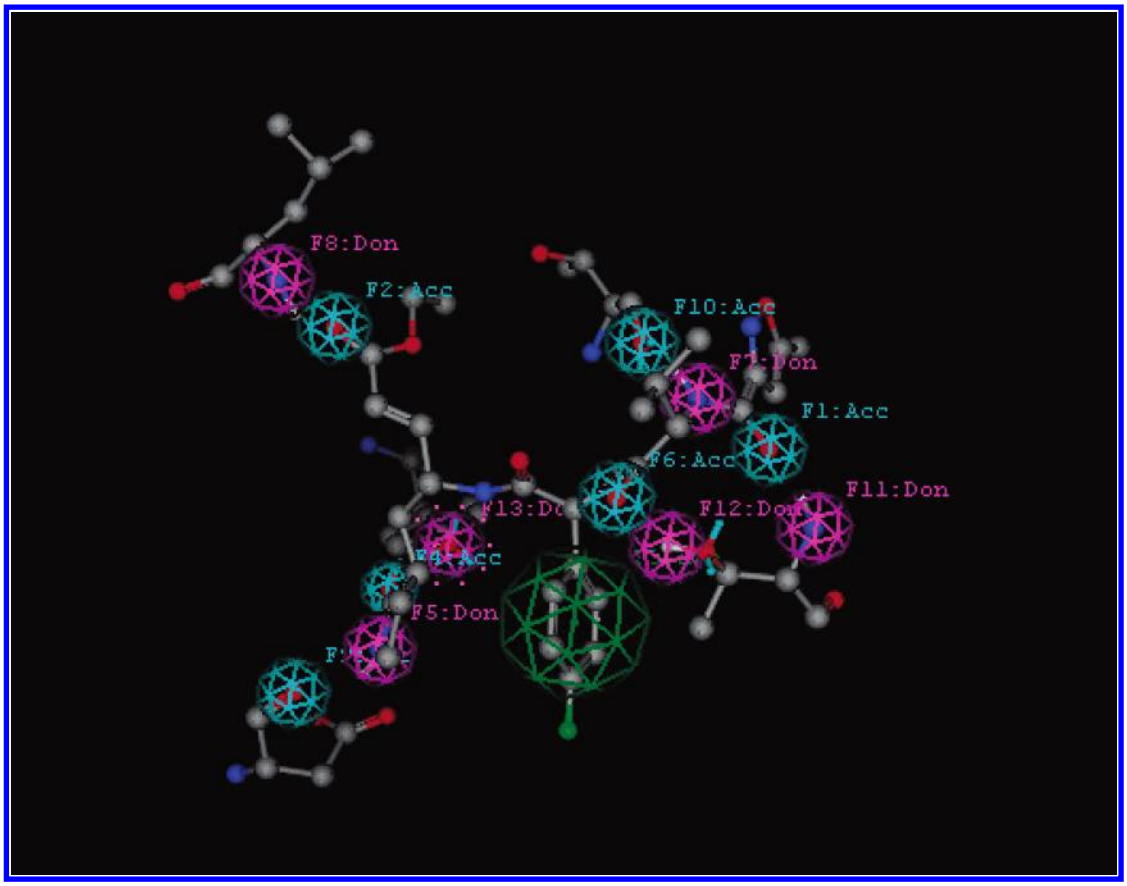

Figure 2. Pharmacophore points for the complex of SARS-CoV and KZ7088. The hydrogen bond donor−acceptor pairs are based on Chou et al.[13] See the legend of Figure 1 for further explanation.

3D Virtual Screening. Given the importance of volume constraint, a 3D search would be more valuable. As a follow-up, we have optimized the 3.6 M compounds in a 3D space. The pharmacophore models thus obtained are displayed in Figures 3 and 4. The first model we used contains the six hydrogen bonds but no aromatic ring. The model permits the retrieval of compounds having five out of the six hydrogen bonds. The results are displayed in Table 4 and correspond to the columns under 3D search without volume constrains. The total number of the unique 3D hits is 7083.

Table 4. 2D and 3D Virtual Screening of SARS-CoV Protease Using KZ7088 Pharmacophore Points

		2D		3D			
				without volume constrains		with volume constrains	
supplier/library	no. of molecules	unique hits	conformers	unique hits	conformers	unique hits	conformers
ACD	87657	5	5	123	142	23	92
Akos OWH	26216	1	1	19	24	5	11
Asinex Gold	194032	50	53	294	482	91	2438
Asinex Platinum	129860	186	217	240	265	55	83
Asinex Preformated	14240	14	14	15	17	1	1
Bionet	35080	0	0	3	3	1	2
Chembridge DVS	30000	0	0	5	5	1	1
Chembridge Express	321716	29	30	171	209	30	126
Chemical Diversity Clab	175551	32	36	255	321	46	152
Chemical Diversity IDC	110484	4	5	133	168	59	306
Chemstar	85981	23	24	131	180	50	415
ChemStar plated	40000	17	18	81	105	30	263
Comgenex	119247	176	176	22	22	3	3
Enamine RS	109695	8	9	8	9	3	3
Enamine S	124420	17	18	292	377	55	246
Evotec	76817	22	22	1273	1543	491	1507
Evotec Screening	122998	147	147	942	1040	158	240
G and J	1867	2	2	1	1	0	0
IBS n	18915	30	59	0	0	0	0
IBS s	173153	86	96	302	451	82	17233
IFlab	109400	22	23	108	125	15	27
Key Organics	34736	0	0	1	1	0	0
Maybridge	75142	5	5	19	76	10	1042
MDPI	9367	12	16	40	88	16	1164
Menai	4512	0	0	5	14	2	46
Nanosyn Explore	18613	5	5	5	5	0	0
Nanosyn Pharma	44000	6	6	31	53	10	123
NCI	250258	334	1054	830	5164	653	47809
Otava	104258	13	15	73	87	30	83
Peakdale	4077	0	0	0	0	0	0
Pharmeks	84143	29	37	101	190	38	11249
Princeton	204215	36	37	262	320	72	538
Ryan Labo	59214	17	57	168	290	104	1374
Sigma Aldrich	58298	86	160	245	3670	221	29681
Sigma Aldrich L	13929	6	7	12	25	3	53
Sigma Aldrich R	69238	56	64	188	162	48	790
Sigma Aldrich S	46284	6	6	47	78	17	568
SPECS	172469	64	69	263	325	61	240
Timtec MaxiVerse	9600	6	8	24	42	5	264
Timtec Stock	100276	15	21	124	167	27	109
Toslab	11743	8	8	23	27	2	6
Tripos	87467	1	1	53	63	16	44
World Molecules	20401	8	8	51	63	23	302
Total	3589569	1584	2539	7083	16506	2589	118695

The total number of 3D conformers is 16 506. The hit ratio is 0.20%. The results thus obtained were refined by adding volume constrains. These constrains correspond to the position of residues that interact directly with KZ7088,[13] as displayed in Figure 4. In this way the hits retrieved will fit the cavity of the enzyme. The 3D results with volume constrains are displayed in the last two columns of Table 4. The total number of unique 3D hits with volume constrains is 2589. The total number of 3D conformers is 118 695. The hit ratio is 0.07%. Finally, the number of compounds satisfying the druggable rules with a scoring value ≥ 0.8 is 1386. Of the 0.07% compounds screened with a hit, 17% have a perfect score of 1.0; while 23% violate one druggable rule (a score of 0.9), 13% violate two rules (a score of 0.8), and 47% have more than two rule violations. The more the violation is, the higher the unlikelihood that the compound can become a drug. Given an allowance of a maximum of two rule violations (i.e., with the requirement for a score of at least 0.8), we obtain that $0.007\% \times (17\% + 23\% + 13\%) = 0.0037\%$ of the original screened compounds are worthy of further tests for biological activities.

Seventh Pharmacophore Point. As can be seen in Figures 3 and 4, the pharmacophore point that corresponds to an aromatic ring at the p-fluorophenyl position was not considered; otherwise not enough hits will have been recovered since it was based on a 3D search. Nevertheless, it is interesting to consider the role of variation at the phenyl position of KZ7088 because this group interacts directly with His-41. The coronavirus family exhibits one main proteinase, described as "3C-like" because the nature of the catalytic site which fulfills a crucial role in the regulation of the virus life-cycle.[12] The catalytic or active site of this enzyme includes Cys and His residues which are considered to be essential for the normal function of the protein. For instance, His-41 interacts directly with the p-fluorophenyl group, and we believe that replacing that group with a hydrogen bond donor group might improve the interaction with the enzyme and in particular will inhibit directly the crucial role of the

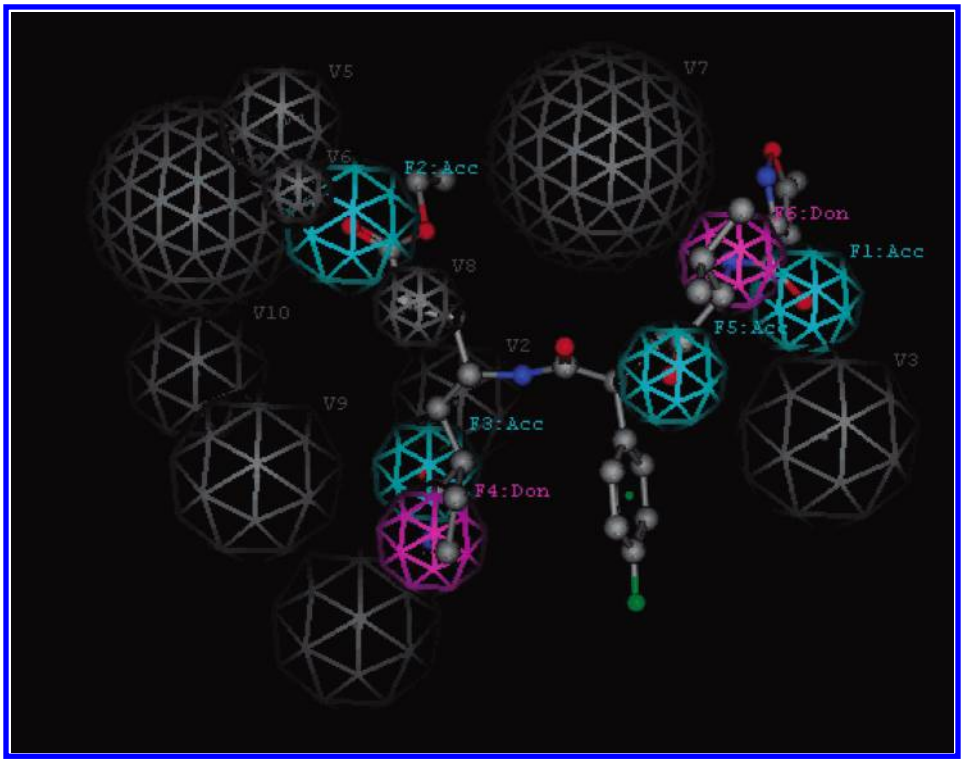

Figure 3. Six hydrogen bond pharmacophore points of KZ7088.[13] See the legend of Figure 1 for further explanation.

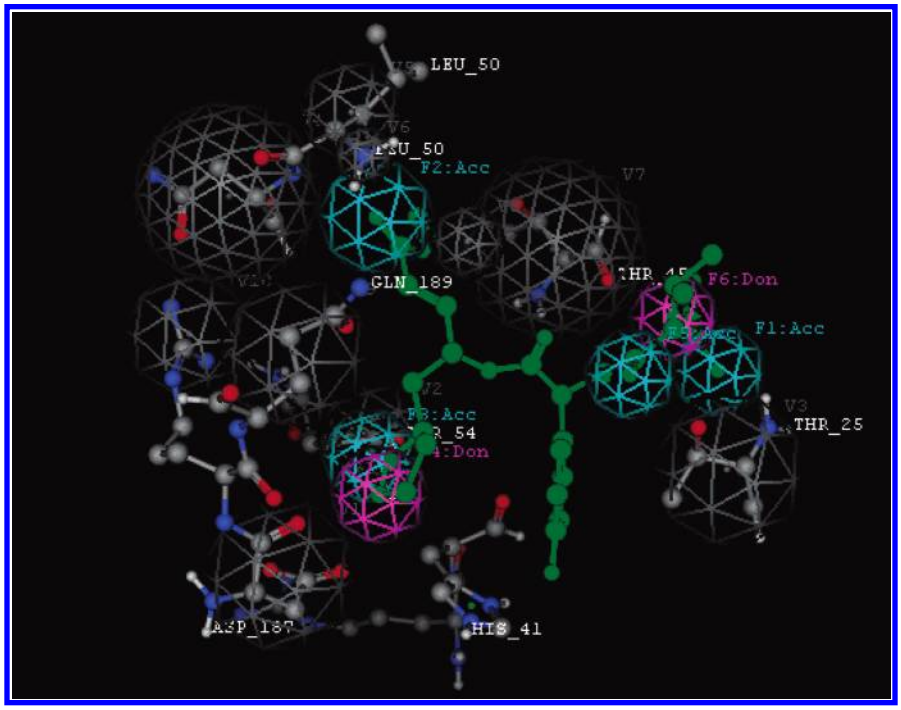

Figure 4. Six hydrogen bond pharmacophore points of KZ7088 surrounded by volume constrains colored in gray. See the legend of Figure 1 for further explanation.

His residue. As shown in Figure 5, replacing a hydrogen atom at the position of the phenyl group with a hydroxyl group will permit formation of a hydrogen bond of about 2 Å with His-41. Further studies in this regard are under way and will be reported elsewhere.

Some Remarks. It is instructive to clarify the following points. **(1)** The current pharmacophore searches were based on the results obtained by docking KZ7088 to the active site of the SARS enzyme conducted by the previous investigators.[13] In this sense, the 3D structure of the SARS-KZ7088 complex has played the role of a "template". With such a template, we can use the pharmacophoric technique to avoid doing a docking study one by one for thousands of different compounds that would otherwise be both time-consuming and costly. This is a remarkable advantage because a set of pharmacophoric features (Figure 1) have been derived from the KZ7088 structure for identifying each of the query compounds for the biological activity. **(2)** The hit is the occurrence of the ligand conformation satisfying a query. A match is the successful mapping of the query features to the

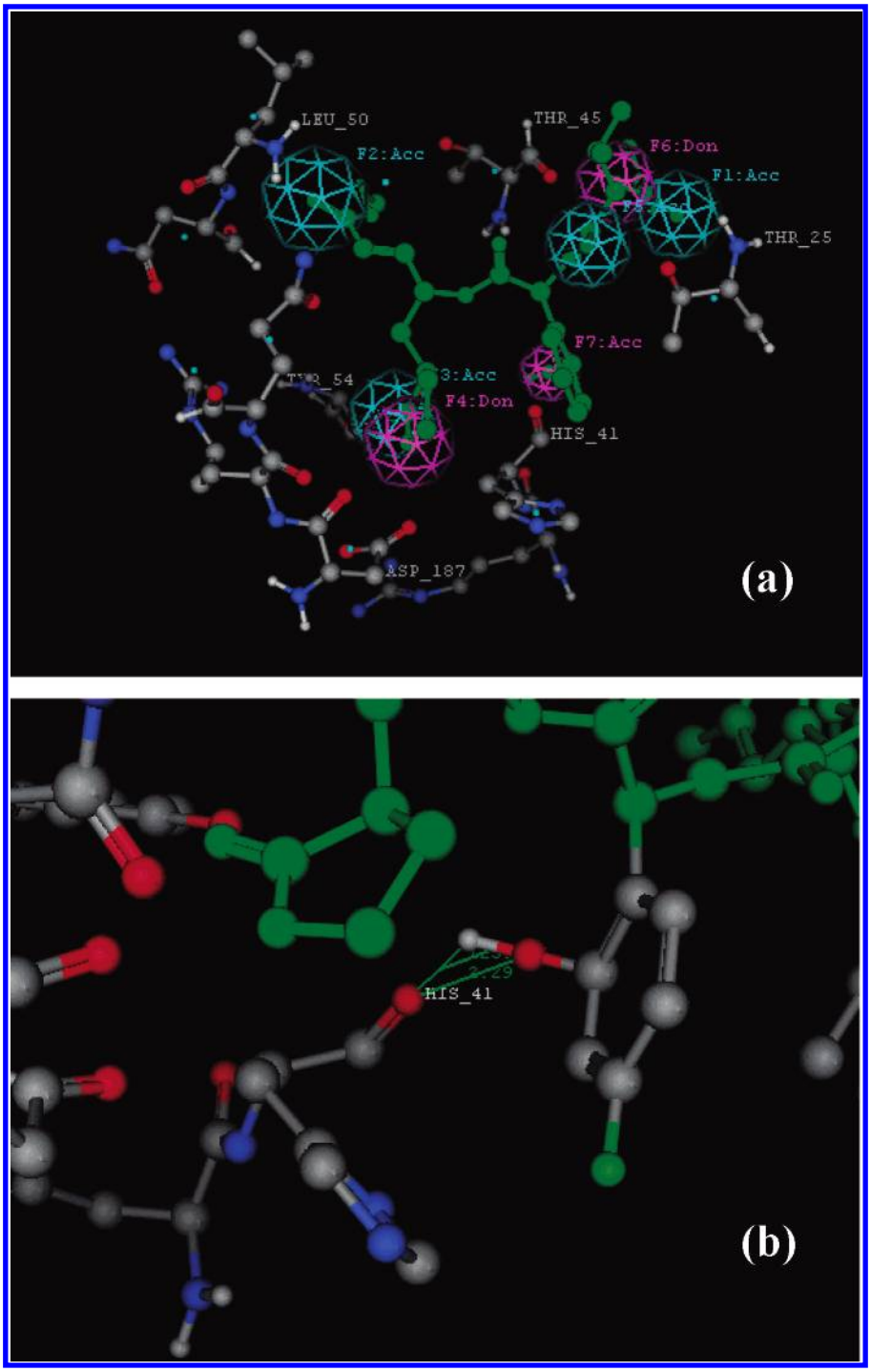

Figure 5. Replace a hydrogen atom at the position of the phenyl group with a hydroxyl group, i.e. add a new pharmacophore point (F7:don) at the p-fluorophenyl position: (a) an overview; (b) a close view, where a detailed interaction between the His-41 and KZ7088 phenyl groups is shown as reflected by forming a hydrogen bond of about 2 Å.

ligand (KZ7088) annotation points. **(3)** The output of the pharmacophore search contains RMSD, i.e., the root-mean-square distance between the query features and their corresponding ligand target points. The smaller the RMSD, the better fitting the query compound has. Listed in Table 5 are the best 500 compounds and the relevant parameters reflecting their druggability. For example, compound 1 satisfies five of the six pharmacophore features;[7] its RMSD is 0.31 with a Drug Score = 0.90; it has 9 hydrogen bond acceptors and 4 hydrogen bond donors; and so forth. This kind of information is very useful for experimental scientists in prioritizing drug candidates.

IV. CONCLUSION

Structure-based design can be performed if the 3D structure of the target molecule is known—for example through X-ray crystallography, NMR (see, e.g., refs 17−19), or homologous modeling (see, e.g., refs 20−23). The structural information is used for building completely novel molecules (de novo design) or to search molecular databases for molecules complementary to the target molecule. Potential drug molecules are evaluated in the binding site using molecular docking (see, e.g., ref 13). The pharmacophore search conducted in this study was based on the atomic

Table 5. Best 500 Compounds Found via the Pharmacophore Searches and Their Parameters Concerned

Hit-Inf [a]	RMSD[b]	drug score[c]	Hacc[d]	Hdon[e]	MW[f]	logP[g]	reactive[h]	Hit-Inf [a]	RMSD[b]	drug score[c]	Hacc[d]	Hdon[e]	MW[f]	logP[g]	reactive[h]
12345	0.310	0.90	9	4	528	0.479	0	12345	0.544	1.00	4	4	411	2.892	0
12356	0.340	0.90	6	4	605	5.949	0	12356	0.545	0.80	6	3	558	5.486	0
12356	0.357	0.80	10	5	569	0.754	1	12346	0.546	0.90	7	3	569	4.517	0
12345	0.363	0.90	7	3	562	2.848	0	12345	0.546	0.90	7	3	511	1.481	0
12346	0.367	0.80	9	8	422	2.263	1	12345	0.548	1.00	8	5	487	2.749	0
12345	0.384	1.00	4	2	391	1.479	0	12345	0.549	0.90	4	3	437	2.378	1
12345	0.404	0.80	3	4	502	4.232	0	12345	0.549	0.90	10	4	658	3.990	0
12356	0.405	0.80	8	8	394	−2.197	0	12345	0.551	0.80	4	5	511	2.141	0
12356	0.409	0.80	8	3	509	−0.189	1	12345	0.551	1.00	9	4	402	−5.680	0
12345	0.413	1.00	8	3	453	−0.719	0	12356	0.551	0.90	7	4	523	2.365	0
12345	0.421	0.80	3	2	630	7.555	0	12345	0.551	1.00	8	4	494	−1.007	0
12345	0.435	0.80	3	4	554	6.587	0	12356	0.551	0.90	7	3	614	3.330	0
12345	0.440	0.90	10	7	440	−0.117	0	12356	0.552	0.90	6	2	513	1.678	0
12345	0.444	0.80	7	6	424	−0.053	1	12356	0.552	0.80	11	8	419	−1.882	0
12345	0.448	0.80	6	4	528	−0.657	1	12345	0.552	1.00	7	3	338	1.726	0
12345	0.452	0.90	7	4	551	4.217	0	12345	0.555	1.00	6	3	468	1.658	0
12345	0.458	1.00	8	3	467	−0.353	0	12345	0.555	0.90	8	4	615	2.198	0
12345	0.464	0.90	10	10	432	−3.890	0	12356	0.556	0.80	6	3	726	8.527	0
12345	0.464	0.90	5	3	510	3.664	0	12345	0.556	0.80	9	4	581	0.666	1
12345	0.470	0.90	6	6	420	3.646	0	12345	0.559	0.90	6	3	511	2.661	0
12345	0.476	0.90	8	4	524	2.500	0	12345	0.559	1.00	3	2	464	3.572	0
12345	0.480	0.90	6	3	557	3.326	0	12345	0.560	0.90	9	4	596	2.195	0
12345	0.481	0.80	3	4	574	6.957	0	12345	0.561	1.00	6	5	361	2.592	0
12345	0.481	0.90	9	3	431	−0.770	1	12345	0.561	0.90	6	3	544	3.555	0
12345	0.486	0.90	6	4	392	1.230	0	12345	0.564	0.90	3	4	527	5.222	0
12345	0.487	1.00	5	3	376	−0.189	0	12345	0.565	0.90	10	5	573	−0.200	0
12345	0.487	0.90	3	4	414	2.820	0	12345	0.566	0.80	8	4	522	−0.371	0
12345	0.488	0.90	4	4	288	−0.557	1	12345	0.566	0.90	8	4	539	0.695	0
12345	0.492	0.90	6	3	544	3.555	0	12345	0.568	0.90	4	2	488	2.818	1
12345	0.495	0.80	5	2	645	4.992	0	12345	0.568	0.80	3	4	524	6.579	0
12345	0.500	0.90	8	3	517	0.870	0	12345	0.570	0.90	9	5	539	−1.929	0
12345	0.500	0.80	15	7	484	−5.369	0	12356	0.570	1.00	7	4	490	1.303	0
12345	0.501	0.90	8	3	530	1.086	0	12345	0.570	1.00	6	5	311	2.378	0
12346	0.502	0.90	7	4	619	4.448	0	12345	0.571	0.90	7	3	555	3.118	0
12345	0.502	1.00	7	4	452	1.212	0	12345	0.571	0.80	5	2	530	2.995	1
12345	0.504	0.90	7	2	543	1.599	0	12356	0.571	0.90	9	4	599	1.149	0
12356	0.505	0.90	9	6	481	−0.750	0	12345	0.574	0.80	8	3	603	2.734	0
12345	0.506	0.90	9	4	571	0.513	0	12345	0.576	1.00	4	5	302	−0.486	0
12345	0.506	0.90	7	3	519	2.418	0	12345	0.576	0.80	9	8	422	2.263	1
12345	0.506	1.00	3	2	466	2.964	0	12356	0.576	0.90	7	2	547	2.331	0
12345	0.507	0.90	5	3	384	2.475	1	12345	0.576	1.00	7	4	457	1.080	0
12345	0.509	0.80	11	7	382	−1.749	0	12345	0.578	0.90	7	6	304	−2.025	0
12345	0.511	0.90	9	3	533	0.641	0	12345	0.579	1.00	4	5	422	1.250	0
12345	0.512	0.90	6	6	269	−0.764	0	12345	0.580	0.90	7	4	551	3.001	0
12345	0.515	1.00	5	3	359	2.324	0	12345	0.581	1.00	4	3	388	3.467	0
12356	0.519	0.90	8	4	589	2.533	0	12356	0.581	0.90	9	3	576	−0.091	0
12345	0.519	0.90	6	4	540	5.227	0	12345	0.582	0.90	8	2	662	4.474	0
12345	0.520	0.80	4	3	397	3.042	1	12345	0.582	1.00	6	4	296	2.796	0
12356	0.520	0.90	7	3	513	1.633	0	12345	0.582	1.00	7	3	491	1.191	0
12345	0.521	0.90	8	4	552	2.396	0	12346	0.583	0.90	7	3	528	1.571	0
12345	0.522	0.90	8	3	611	3.118	0	12345	0.584	0.80	8	3	536	−0.357	1
12345	0.524	1.00	7	4	465	1.557	0	12356	0.584	0.90	8	3	542	0.338	0
12356	0.524	0.90	9	3	548	0.699	0	12346	0.584	1.00	3	3	397	1.798	0
12345	0.524	0.90	4	4	400	2.820	0	12345	0.585	0.90	9	3	524	−1.285	0
12345	0.525	0.80	5	2	589	3.770	0	12345	0.586	1.00	6	2	481	3.755	0
12345	0.527	0.90	7	4	527	1.855	0	12345	0.587	0.80	8	6	334	−2.304	1
12345	0.528	0.90	4	2	437	2.618	1	12356	0.587	1.00	6	5	358	1.037	0
12346	0.528	0.80	11	5	637	2.385	0	12345	0.587	0.80	7	4	425	−0.076	1
12345	0.528	1.00	6	3	481	2.570	0	12345	0.588	0.80	5	4	559	4.418	1
12345	0.529	1.00	10	4	478	−0.934	0	12345	0.588	0.90	7	7	299	−1.403	0
12356	0.529	1.00	7	3	478	2.850	0	12356	0.589	0.90	5	4	590	4.499	0
12356	0.532	0.90	5	3	543	3.866	0	12345	0.590	0.90	9	4	597	0.178	0
12345	0.532	0.90	8	8	420	2.389	0	12345	0.590	1.00	5	4	347	1.631	0
12345	0.533	1.00	5	5	417	0.584	0	12345	0.591	0.90	8	4	676	5.845	0
12345	0.534	0.90	8	6	300	−0.398	0	12345	0.592	1.00	5	4	365	1.193	0
12345	0.534	0.80	4	3	543	4.598	0	12356	0.592	0.90	8	3	528	0.114	0
12345	0.535	0.80	4	3	561	4.367	0	12345	0.592	1.00	6	3	485	0.919	0
12356	0.535	0.80	8	6	526	3.838	0	12356	0.595	0.90	7	2	551	2.112	0
12345	0.535	0.80	9	4	575	−0.834	0	12345	0.596	0.90	6	2	656	4.635	0
12356	0.539	0.90	8	2	573	2.243	0	12345	0.596	0.80	15	8	483	−4.918	0
12345	0.540	0.90	7	3	519	2.418	0	12345	0.597	0.90	8	3	580	2.366	0
12345	0.541	0.80	16	4	574	−3.401	0	12345	0.597	0.80	5	3	685	6.369	0
12345	0.542	0.90	5	2	559	4.517	0	12356	0.598	0.90	9	6	481	−0.750	0

Table 5 (Continued)

Hit-Inf [a]	RMSD[b]	drug score[c]	Hacc[d]	Hdon[e]	MW[f]	logP[g]	reactive[h]	Hit-Inf [a]	RMSD[b]	drug score[c]	Hacc[d]	Hdon[e]	MW[f]	logP[g]	reactive[h]
12345	0.542	0.80	10	3	573	0.054	0	12345	0.598	1.00	7	3	489	0.801	0
12345	0.543	1.00	7	4	477	0.727	0	12345	0.599	1.00	6	4	367	0.381	0
12356	0.600	0.90	6	2	544	2.684	0	12345	0.636	1.00	5	2	476	2.724	0
12345	0.600	1.00	4	2	430	3.833	0	12345	0.636	1.00	5	3	370	0.420	0
12345	0.601	1.00	5	3	429	1.848	0	12345	0.636	0.90	9	8	358	1.710	0
12345	0.601	1.00	7	5	364	−1.485	0	12345	0.636	0.80	6	4	662	5.805	0
12345	0.601	1.00	5	3	459	2.815	0	12345	0.637	0.90	6	2	380	0.134	1
12345	0.601	0.80	7	3	530	1.163	1	12345	0.637	1.00	7	3	373	0.671	0
12345	0.602	0.80	12	11	360	−7.056	0	12345	0.638	0.90	5	3	541	3.141	0
12345	0.602	0.80	12	11	360	−7.056	0	12345	0.638	1.00	4	2	469	2.623	0
12356	0.603	1.00	7	4	470	4.391	0	12345	0.638	1.00	8	4	482	−1.007	0
12345	0.604	0.80	8	2	762	3.559	0	12345	0.638	0.90	8	3	615	3.020	0
12345	0.605	0.80	8	4	510	−0.371	0	12345	0.638	0.90	4	3	522	4.203	0
12345	0.606	0.90	4	2	532	4.250	0	12345	0.638	0.90	5	3	573	4.709	0
12345	0.607	1.00	5	2	360	1.074	0	12345	0.638	1.00	6	4	429	0.957	0
12346	0.608	0.80	8	6	572	1.658	0	12345	0.638	1.00	5	4	481	4.821	0
12345	0.608	1.00	5	3	490	3.319	0	12345	0.638	1.00	7	4	422	0.833	0
12356	0.609	0.90	8	4	568	2.188	0	12345	0.639	1.00	10	5	347	−2.886	0
12345	0.609	0.80	4	4	515	6.131	0	12345	0.639	1.00	10	5	347	−2.886	0
12356	0.609	0.80	6	4	585	4.768	0	12356	0.639	1.00	7	3	479	1.047	0
12345	0.609	0.80	8	8	368	−1.186	0	12345	0.639	1.00	7	4	426	2.845	0
12345	0.610	1.00	7	3	451	0.411	0	12345	0.639	0.90	6	3	583	4.110	0
12345	0.611	1.00	6	4	435	2.147	0	12345	0.639	0.90	4	2	531	4.343	0
12345	0.611	0.90	8	4	521	0.720	0	12345	0.640	1.00	5	3	471	4.618	0
12345	0.611	0.90	7	5	511	0.157	0	12345	0.640	0.90	8	4	615	2.198	0
12356	0.612	1.00	7	4	432	2.724	0	12345	0.640	0.90	5	7	235	−1.097	0
12345	0.612	1.00	7	4	418	2.415	0	12345	0.641	0.80	10	3	573	0.197	0
12345	0.613	0.90	8	3	536	0.115	0	12345	0.641	0.90	9	4	576	1.381	0
12345	0.614	0.90	8	4	512	1.243	0	12345	0.642	0.80	5	2	631	5.272	0
12345	0.615	0.80	8	5	505	−0.209	1	12345	0.642	1.00	5	3	376	−0.189	0
12345	0.615	0.80	5	5	658	5.913	0	12345	0.642	1.00	5	5	435	1.546	0
12345	0.615	0.80	7	3	546	1.607	1	12345	0.642	0.80	4	3	552	4.239	0
12346	0.618	0.90	9	6	453	−1.367	0	12345	0.643	1.00	5	5	237	1.188	0
12345	0.618	0.80	7	3	544	1.553	1	12345	0.643	0.80	7	6	507	5.469	0
12356	0.619	0.80	8	2	588	3.728	1	12346	0.644	0.80	8	4	530	2.758	0
12456	0.620	0.90	6	3	471	1.989	0	12345	0.644	0.90	5	3	384	2.475	1
12345	0.620	1.00	7	3	477	0.801	0	12346	0.644	0.80	8	6	517	0.029	0
12345	0.620	0.80	4	5	591	5.201	0	12345	0.645	0.90	7	4	455	1.284	1
12345	0.621	0.80	6	2	624	4.388	0	12345	0.645	0.80	9	4	548	−0.995	1
12345	0.621	0.80	10	3	623	1.419	0	12345	0.647	1.00	5	4	492	3.326	0
12345	0.621	1.00	4	4	304	1.779	0	12345	0.647	0.90	6	3	504	1.206	0
12345	0.621	0.90	11	5	426	−4.423	0	12356	0.647	0.90	8	4	598	4.109	0
12345	0.622	1.00	6	4	392	0.536	0	12356	0.647	0.90	8	2	563	1.568	0
12345	0.623	1.00	4	2	462	3.782	0	12345	0.647	0.90	7	5	522	4.928	0
12345	0.624	1.00	4	2	497	3.886	0	12345	0.647	0.90	9	3	554	0.966	0
12345	0.624	0.90	8	4	543	1.449	0	12345	0.648	0.90	7	3	517	1.581	0
12345	0.625	0.90	8	6	380	−2.512	0	12345	0.648	0.80	13	5	614	3.345	0
12345	0.625	1.00	4	3	372	2.903	0	12346	0.648	0.80	4	5	575	5.675	0
12345	0.625	0.90	10	10	432	−3.890	0	12345	0.649	0.90	6	2	427	0.756	1
12345	0.625	1.00	6	3	447	2.597	0	12345	0.649	1.00	5	4	461	3.727	0
12345	0.625	0.80	6	6	364	1.365	0	12345	0.649	1.00	6	4	435	2.292	0
12346	0.626	0.80	10	6	445	−2.532	1	12345	0.649	0.80	6	4	554	2.873	1
12345	0.626	1.00	8	2	400	−0.274	0	12345	0.649	0.90	8	4	500	−0.223	0
12345	0.626	0.90	5	6	486	2.905	0	12345	0.650	0.90	6	3	511	2.493	0
12345	0.626	1.00	7	5	278	−2.076	0	12345	0.651	1.00	5	5	237	1.188	0
12356	0.627	0.80	8	2	584	2.882	1	12345	0.651	1.00	4	3	402	4.313	0
12345	0.627	0.90	7	4	502	2.588	0	12356	0.651	0.90	8	3	578	1.395	0
12345	0.628	0.80	9	3	525	−0.810	1	12345	0.652	0.90	8	4	518	0.823	0
12345	0.628	1.00	7	5	277	−0.100	0	12345	0.652	1.00	10	4	362	−4.030	0
12356	0.628	0.90	7	3	645	5.402	0	12345	0.653	0.90	9	5	523	−1.866	0
12345	0.628	0.90	7	4	544	2.472	0	12345	0.653	0.80	8	3	509	−0.046	1
12345	0.629	0.90	8	3	518	0.919	0	12345	0.654	0.90	6	3	537	3.025	0
12356	0.631	0.90	7	4	547	2.842	0	12345	0.655	0.80	3	4	559	7.232	0
12345	0.631	1.00	6	4	491	3.106	0	12356	0.655	0.90	8	3	542	0.338	0
12345	0.631	1.00	6	2	322	3.796	0	12345	0.656	0.90	4	4	526	2.427	0
12345	0.632	0.80	12	6	425	−3.680	0	12345	0.656	0.90	8	4	571	2.085	0
12345	0.633	0.90	7	3	559	1.036	0	12345	0.656	1.00	7	4	461	1.151	0
12345	0.633	0.90	7	3	612	2.359	0	12345	0.656	1.00	7	3	404	0.355	0
12345	0.633	0.80	10	6	541	−0.064	0	12345	0.657	0.80	6	5	665	4.956	0
12345	0.633	0.80	10	6	541	−0.064	0	12345	0.657	0.90	10	10	432	−3.890	0
12356	0.633	0.90	7	3	541	2.414	0	12345	0.657	1.00	5	3	470	4.513	0
12346	0.634	0.80	9	2	548	2.292	0	12345	0.657	1.00	6	4	490	0.958	0
12346	0.635	0.80	6	3	601	5.702	0	12356	0.657	1.00	6	3	482	2.366	0

Table 5 (Continued)

Hit-Inf [a]	RMSD[b]	drug score[c]	Hacc[d]	Hdon[e]	MW[f]	logP[g]	reactive[h]	Hit-Inf [a]	RMSD[b]	drug score[c]	Hacc[d]	Hdon[e]	MW[f]	logP[g]	reactive[h]
12356	0.635	0.90	7	3	501	1.633	0	12345	0.657	1.00	4	3	319	−0.691	0
12345	0.635	0.80	6	4	550	4.295	0	12346	0.658	0.80	9	3	602	2.691	0
12345	0.635	0.90	4	4	410	0.755	1	12356	0.658	0.80	6	2	512	3.456	0
12345	0.636	0.90	4	3	576	4.420	0	12456	0.658	0.90	6	2	544	2.684	0
12345	0.659	0.90	5	4	568	4.701	0	12356	0.682	0.90	9	7	443	−0.869	0
12345	0.659	0.90	8	4	633	3.613	0	12356	0.682	0.80	10	3	579	0.018	1
12345	0.660	0.90	3	4	338	0.919	0	12345	0.683	0.90	7	3	479	−0.109	1
12356	0.660	0.90	5	4	516	3.671	0	12345	0.683	0.90	5	7	253	−3.317	0
12345	0.660	1.00	6	3	396	1.565	0	12356	0.683	0.80	5	3	606	5.320	0
12356	0.661	0.80	11	9	406	−3.461	0	12345	0.683	1.00	5	3	451	3.921	0
12345	0.661	0.80	6	2	695	5.933	0	12345	0.683	0.80	7	4	613	1.978	1
12345	0.661	0.90	8	4	481	−0.922	1	12345	0.683	1.00	6	3	494	2.190	0
12345	0.661	0.90	9	3	573	−0.984	0	12345	0.684	1.00	5	2	433	1.664	0
12356	0.661	1.00	8	4	417	0.028	0	12345	0.684	0.80	6	4	642	2.972	0
12345	0.661	0.80	6	3	662	5.612	0	12356	0.684	1.00	7	3	491	1.213	0
12345	0.661	1.00	7	3	498	1.579	0	12345	0.684	0.90	9	3	597	1.000	0
12345	0.661	1.00	6	3	441	1.198	0	12345	0.684	0.90	8	3	592	1.703	0
12345	0.661	1.00	5	3	402	3.311	0	12345	0.684	0.80	4	4	614	5.721	0
12345	0.662	1.00	5	3	468	3.157	0	12345	0.685	0.90	10	5	569	2.061	0
12345	0.662	0.90	7	4	557	5.136	0	12345	0.685	0.90	10	5	569	2.061	0
12345	0.662	0.90	6	3	630	4.797	0	12345	0.685	0.80	5	4	503	3.088	0
12345	0.662	0.90	8	4	534	1.267	0	12345	0.685	0.90	7	3	505	1.437	0
12345	0.662	0.90	6	4	520	3.113	0	12356	0.686	0.90	8	6	417	−0.844	0
12345	0.663	0.90	5	3	569	4.997	0	12345	0.686	0.90	9	4	571	0.513	0
12345	0.663	1.00	5	4	361	2.292	0	12345	0.686	0.80	10	3	649	1.952	0
12345	0.663	1.00	5	4	391	1.087	0	12345	0.687	1.00	4	2	458	2.274	0
12345	0.664	1.00	8	4	480	−1.576	0	12345	0.687	0.90	3	3	481	4.305	0
12345	0.664	1.00	5	4	326	1.164	0	12345	0.688	1.00	7	3	491	1.511	0
12345	0.664	0.90	5	3	498	3.992	1	12345	0.688	1.00	5	4	430	3.760	0
12345	0.665	0.90	7	4	557	2.532	0	12345	0.688	0.80	3	4	508	3.635	0
12345	0.665	0.90	6	6	395	0.675	0	12345	0.688	1.00	5	2	475	3.147	0
12345	0.666	0.90	7	3	595	4.488	0	12345	0.689	0.90	8	3	546	1.710	0
12345	0.666	0.80	5	4	554	4.535	1	12345	0.689	0.90	5	3	515	2.881	0
12356	0.666	0.90	5	1	508	3.622	0	12345	0.689	0.80	6	2	532	3.117	0
12345	0.666	0.90	11	5	481	−6.392	0	12345	0.689	0.80	5	4	547	4.246	0
12345	0.667	0.90	6	5	435	0.908	1	12345	0.689	1.00	5	2	459	1.936	0
12345	0.668	0.90	6	3	517	3.897	0	12356	0.689	0.90	9	4	524	−1.238	0
12345	0.668	1.00	6	5	474	3.049	0	12356	0.690	1.00	4	3	410	1.347	0
12356	0.669	0.90	7	2	609	3.688	0	12345	0.690	0.90	5	2	531	4.128	0
12345	0.669	0.90	8	6	396	−2.549	0	12345	0.691	0.90	10	3	576	0.993	0
12345	0.670	0.80	6	2	684	4.406	0	12356	0.691	0.90	7	2	515	2.931	0
12346	0.671	0.80	4	6	440	2.388	0	12345	0.691	0.80	6	4	604	1.481	0
12345	0.671	0.90	8	3	556	2.513	0	12356	0.691	0.90	7	3	596	3.415	0
12345	0.671	1.00	6	4	420	3.872	0	12345	0.691	0.90	6	3	541	2.632	0
12345	0.671	0.80	8	4	592	0.471	0	12345	0.692	1.00	4	5	434	1.023	0
12345	0.671	0.90	8	4	613	5.268	0	12345	0.692	0.90	8	8	480	3.890	0
12345	0.671	1.00	6	5	456	2.594	0	12345	0.692	0.80	10	3	659	1.826	0
12345	0.671	1.00	7	4	499	0.382	0	12345	0.692	0.80	6	4	604	1.481	0
12345	0.672	1.00	6	5	311	1.213	0	12356	0.692	0.90	8	3	550	1.729	0
12356	0.672	0.90	7	4	528	3.871	0	12345	0.693	0.90	8	6	380	−2.512	0
12345	0.672	0.80	9	3	562	0.073	1	12345	0.693	1.00	6	2	349	0.789	0
12345	0.672	0.90	6	2	636	3.826	0	12345	0.694	0.90	7	4	501	1.680	0
12345	0.672	1.00	5	3	464	3.116	0	12345	0.694	0.90	6	4	539	2.037	0
12345	0.673	0.80	10	4	559	−0.124	0	12346	0.694	0.90	5	4	527	3.220	0
12345	0.673	0.90	5	4	545	4.587	0	12345	0.694	1.00	6	3	335	1.139	0
12345	0.673	1.00	10	4	404	−1.855	0	12356	0.695	0.80	7	4	538	5.096	0
12345	0.673	0.80	5	2	602	3.828	0	12345	0.695	1.00	4	4	373	1.790	0
12345	0.673	0.90	8	3	548	0.259	0	12345	0.695	1.00	4	2	497	5.613	0
12346	0.674	1.00	8	4	472	2.180	0	12356	0.695	0.80	8	3	523	0.200	1
12345	0.674	0.90	4	5	456	1.142	0	12345	0.696	0.80	6	3	578	4.155	1
12345	0.674	1.00	6	4	459	4.828	0	12345	0.696	1.00	6	3	479	2.626	0
12345	0.674	0.90	6	4	545	5.399	0	12356	0.696	1.00	6	5	381	−0.150	0
12345	0.676	1.00	4	5	378	1.650	0	12345	0.697	0.90	9	3	548	0.699	0
12345	0.677	1.00	5	4	385	2.124	0	12345	0.697	0.80	14	8	423	−5.989	0
12356	0.677	0.90	8	3	542	0.338	0	12345	0.697	0.90	9	4	548	−0.123	0
12346	0.677	0.90	5	4	561	4.793	0	12345	0.697	1.00	7	5	473	1.050	0
12345	0.678	0.90	8	3	516	−0.052	0	12345	0.697	0.90	6	3	545	4.443	0
12345	0.678	0.80	11	5	568	−1.337	0	12356	0.697	0.80	9	3	511	−1.200	1
12345	0.678	1.00	4	3	460	2.153	0	12345	0.697	0.90	6	5	494	2.460	0
12345	0.679	1.00	5	3	457	1.891	0	12345	0.697	0.90	8	4	585	2.632	0
12345	0.679	0.90	8	7	381	−0.714	0	12345	0.698	0.90	6	5	494	3.414	0
12356	0.679	0.80	9	4	624	2.488	0	12345	0.698	0.80	6	3	500	2.576	0
12345	0.680	0.90	8	4	518	0.976	0	12345	0.698	1.00	8	3	493	0.037	0

Table 5 (Continued)

Hit-Inf [a]	RMSD[b]	drug score[c]	Hacc[d]	Hdon[e]	MW[f]	logP[g]	reactive[h]	Hit-Inf [a]	RMSD[b]	drug score[c]	Hacc[d]	Hdon[e]	MW[f]	logP[g]	reactive[h]
12345	0.680	1.00	4	4	447	1.861	0	12345	0.698	0.90	10	6	426	−3.532	0
12345	0.680	0.90	8	3	524	1.197	0	12345	0.698	1.00	6	4	433	0.856	0
12345	0.681	0.90	7	7	299	−1.403	0	12345	0.699	0.90	6	4	542	3.483	0
12345	0.681	0.80	4	4	549	4.815	1	12345	0.699	0.80	6	6	390	−0.468	1
12345	0.681	0.80	6	4	593	2.514	0	12345	0.699	1.00	5	4	380	2.340	0
12346	0.682	0.90	6	3	548	3.162	0	12345	0.699	0.80	8	6	550	0.867	0
12345	0.699	0.80	10	5	609	2.984	0	12345	0.707	1.00	10	5	395	−2.450	0
12345	0.699	0.80	10	2	684	0.297	0	12345	0.707	1.00	8	4	495	0.187	0
12345	0.700	1.00	6	4	407	2.549	0	12345	0.707	0.80	6	2	543	3.395	0
12345	0.700	1.00	6	5	342	1.100	0	12345	0.708	0.80	6	2	588	3.307	0
12346	0.700	0.80	10	10	431	−2.370	1	12345	0.708	0.90	8	3	556	0.383	0
12345	0.701	0.80	7	3	512	0.953	1	12345	0.709	0.90	6	3	565	3.900	0
12345	0.701	0.90	5	3	504	2.915	0	12345	0.709	1.00	5	4	492	3.326	0
12345	0.701	1.00	3	2	446	2.919	0	12345	0.711	0.90	3	4	510	2.513	0
12345	0.701	0.80	5	2	675	5.057	0	12345	0.711	1.00	5	3	348	−0.044	0
12345	0.702	1.00	4	4	469	3.738	0	12345	0.711	0.90	11	5	481	−6.392	0
12345	0.702	1.00	9	4	301	−1.388	0	12345	0.711	1.00	7	4	432	1.114	0
12356	0.702	0.90	7	4	516	1.835	0	12356	0.712	0.80	11	5	637	2.385	0
12345	0.702	0.90	4	2	533	4.367	0	12345	0.712	0.90	7	3	554	1.937	0
12346	0.702	0.80	9	8	422	2.263	1	12345	0.712	1.00	7	4	446	3.914	0
12345	0.702	0.80	8	3	513	0.348	1	12345	0.713	0.80	4	2	538	4.827	1
12345	0.703	0.80	9	8	422	2.263	1	12345	0.713	0.80	6	2	658	3.647	1
12345	0.703	1.00	7	5	465	0.926	0	12345	0.713	0.80	11	8	491	−2.433	0
12345	0.704	0.90	8	3	592	1.703	0	12345	0.714	0.90	4	3	501	4.732	0
12345	0.704	0.80	13	6	427	−3.791	0	12356	0.714	1.00	7	3	492	−0.194	0
12345	0.705	0.80	9	6	616	0.039	0	12345	0.714	1.00	4	2	412	2.402	0
12346	0.705	0.90	8	6	483	−1.371	0	12345	0.714	0.80	8	3	521	−0.046	1
12345	0.705	0.90	9	8	458	2.329	0	12345	0.714	0.80	7	4	487	0.757	1
12345	0.706	1.00	5	4	391	1.110	0	12345	0.715	0.90	6	6	269	−0.764	0
12345	0.706	1.00	6	2	442	0.797	0	12345	0.715	0.90	5	3	505	2.596	0
12346	0.706	0.90	7	6	360	1.761	0	13456	0.715	0.90	6	2	588	2.750	0

[a] The hit information is defined according to the Lipinski's rule of five.[7] [b] The root-mean-square distance between the query features and their corresponding ligand target points. [c] Computed according to eq 2. [d] Hydrogen bond acceptor; see eq 1 and ref 7. [e] Hydrogen bond donor; see eq 1 and ref 7. [f] Molecular weight; see eq 1 and ref 7. [g] The logarithm of the octanol/water partition coefficient; see eq 1 and ref 7. [h] See eq 1 and ref 7.

coordinates of the complex obtained by docking KZ7088 to SARS CoV M^{pro}.[13] The resulting pharmacophore models provide very useful information about the chemical features that interact with the active site residues. It also provides a unique featured template to test if a given synthesis candidate can assume the optimal geometry and display chemical functionality necessary to fit the model features. In the current study, the hydrogen bond donor and acceptor were chosen for pharmacophore modeling. Of course, one can also choose some other features for modeling, such as aromatic ring, hydrophobic aromatic, hydrophobic aliphatic, positive charge, negative charge, hydrogen bond acceptor lipid, positive ionizable, and negative ionizable. Meanwhile the following remarkable benefits from pharmacophore modeling have been explicitly demonstrated through the present study: **(1)** providing useful information of the chemical functionality and orientation to help make a better choice for synthesizing compounds; **(2)** gaining insight into common chemical features that are considered responsible for ligand−receptor binding affinity; **(3)** significantly reducing the scope of compounds for further studies; and **(4)** developing useful featured templates for faster lead finding and optimization.

REFERENCES AND NOTES

(1) Oba, Y., The use of corticosteroids in SARS. *New Engl. J. Med.* **2003**, *348*, 2034.
(2) Anthrax, *http://www.chem.ox.ac.uk/anthrax/results.htm*, 2002.
(3) Richards, W. G. Virtual screening using grid computing: the screensaver project. *Nature Rev. Drug Discovery* **2002**, *1*, 551.
(4) Ajay, A.; Walters, W. P.; Murcko, M. A. Can we learn to distinguish between "drug-like" and "nondrug-like" molecules? *J. Med. Chem.* **1998**, *41*, 3314.
(5) Rishton, G. M. Nonleadlikeness and leadlikeness in biochemical screening. *Drug Discovery Today* **2003**, *8*, 86.
(6) Sadowski, J.; Kubinyi, H. A scoring scheme for discriminating between drugs and nondrugs. *J. Med. Chem.* **1998**, *41*, 3325.
(7) Lipinski, C. A. Drug-like properties and the causes of poor solubility and poor permeability, *J. Pharmacol. Toxicol. Methods* **2000**, *44*, 235.
(8) Xu, J.; Stevenson, J. Drug-like index: a new approach to measure drug-like compounds and their diversity. *J. Chem. Inf. Comput. Sci.* **2000**, *40*, 1177.
(9) Oprea, T. I. Property distribution of drug-related chemical databases. *J. Comput.-Aided Mol. Des.* **2000**, *14*, 251.
(10) Rishton, G. M. Reactive compounds and in vitro false positives in HTS, *Drug Discovery Today* **1997**, *2*, 382.
(11) Baurin, N. Etude et développement de techniques QSAR pour la recherche de molécules d'intérêts thérapeutique, Criblage virtuel et Analyse de chmiothèque, Université d'Orléans, 2002.
(12) Anand, K.; Ziebuhr, J.; Wadhwani, P.; Mesters, J. R.; Hilgenfeld, R.; Coronavirus main proteinase (3CLpro) structure: basis for design of anti-SARS drugs. *Science* **2003**, *300*, 1763.
(13) Chou, K. C.; Wei, D. Q.; Zhong, W. Z. Binding mechanism of coronavirus main proteinase with ligands and its implication to drug design against SARS. *Biochem. Biophys. Res. Comm.* **2003**, *308*, 148 (Erratum: ibid. **2003**, *310*, 675).
(14) Wildman, S. A.; Crippen, G. M. Prediction of physicochemical parameters by atomic contributions. *J. Chem. Inf. Comput. Sci.* **1999**, *39*, 868.
(15) Group, C. C. MOE, H3A 2R7, Montreal, Canada. 2002.
(16) WDI, *World Drug Index*; 14 Great Queen Street, London, WC2B 5DF, UK.
(17) Chou, J. J.; Matsuo, H.; Duan, H.; Wagner, G. Solution structure of the RAIDD CARD and model for CARD/CARD interaction in caspase-2 and caspase-9 recruitment. *Cell* **1998**, *94*, 171.
(18) Chou, J. J.; Li, H.; Salvesen, G. S.; Yuan, J.; Wagner, G. Solution structure of BID, an intracellular amplifier of apoptotic signaling. *Cell* **1999**, *96*, 615.

(19) Chou, J. J.; Li, S.; Klee, C. B.; Bax, A. Solution structure of Ca2+-calmodulin reveals flexible hand-like properties of its domains. *Nature Struct. Biol.* **2001**, *8*, 990.
(20) Chou, K. C. The convergence-divergence duality in lectin domains of the selectin family and its implications. *FEBS Lett.* **1995**, *363*, 123.
(21) Chou, K. C.; Watenpaugh, K. D.; Heinrikson, R. L. A Model of the complex between cyclin-dependent kinase 5(Cdk5) and the activation domain of neuronal Cdk5 activator. *Biochem. Biophys. Res. Commun.* **1999**, *259*, 420.
(22) Chou, K. C.; Tomasselli, A. G.; Heinrikson, R. L. Prediction of the Tertiary Structure of a Caspase-9/Inhibitor Complex. *FEBS Lett.* **2000**, *470*, 249.
(23) Chou, K. C.; Howe, W. J. Prediction of the tertiary structure of the beta-secretase zymogen. *Biochem. Biophys. Res. Commun.* **2002**, *292*, 702.

CI034270N